JOC The Journal of Organic Chemistry

Article

pubs.acs.org/joc

Synthesis, Characterization, Physical Properties, and OLED Application of Single BN-Fused Perylene Diimide

Gang Li,[†,‡] Yongbiao Zhao,[§] Junbo Li,[†] Jun Cao,[∥] Jia Zhu,[∥] Xiao Wei Sun,*[,§] and Qichun Zhang*[,†]

[†]School of Materials Science Engineering, Nanyang Technological University, 639798, Singapore

[‡]Beijing National Laboratory for Molecular Sciences (BNLMS), Institute of Chemistry, Chinese Academy of Sciences, 100190 Beijing, P. R. China

[§]School of Electrical and Electronic Engineering, Nanyang Technological University, 639798, Singapore

[∥]Key Laboratory of Theoretical and Computational Photochemistry, Ministry of Education, College of Chemistry, Beijing Normal University, 100875 Beijing, China

Supporting Information

ABSTRACT: It is very challenging to introduce azaborine into an electron-deficient arene system because of unfavorable intramolecular electrophilic borylation reaction. In this report, we adopted a straightforward methodology to construct a large BN-embedded π-system based on perylene diimide (PDI), which is the first BN-annulation example with highly electron-withdrawing polycyclic aromatic hydrocarbons. The physical properties of the as-prepared *N*,*N*-dicyclohexyl-1-aza-12-bora-benzoperylene diimide (**PDI-1BN**) have been fully studied, and its sensing behavior to fluoride ion as well as its OLED performance was also investigated.

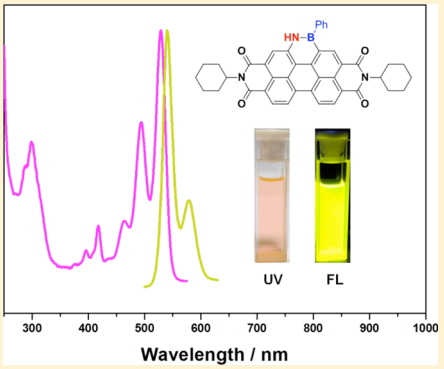

INTRODUCTION

In the past decades, significant progresses have been witnessed in polycyclic aromatic hydrocarbons (PAHs) due to their interesting physical properties and potential applications in organic electronics.[1−14] Among all members of the PAH family, perylene diimide (PDI) derivatives have been studied more extensively[15] because of their rigid planar backbones and extended π-conjugation, which exhibit high charge-carrier mobility, intense luminescence, extraordinary thermal and photochemical stability, and unique self-assembly behaviors.[16] In addition, PDIs have been widely employed as promising active elements in photovoltaic devices,[17−19] organic field effect transistors (OFETs),[20−23] and electrophotographic devices.[24] In order to further improve the properties of the PDIs, developing core-extended PDIs has been strongly sought.[25−32] Typically, incorporating main group elements into extended-PDI frameworks has been extensively explored in the past decade,[33−35] and a large number of PDI derivatives decorated with diverse heterocycles such as sulfur-, thiophene-, and N-heterocycles in the bay regions have been demonstrated.[36−42]

Recently, the replacement of the C═C bond with one isoelectronic and isosteric B-N fragment in PAHs has been demonstrated to display obvious different electronic properties comparing with their all-carbon analogues.[43−46] In addition, the aromaticity of PAHs can stabilize the BN unit and the planarity of PAHs is enforced by this unsaturated ring system.[47−49] Especially, the different electronegativities between boron (B, 2.0) and nitrogen elements (N, 3.0) in the BN unit have a big contribution to the molecular frontier orbitals and intermolecular interactions of PAHs.[45] Nakamura and co-workers reported a BN-fused PAH, which exhibited higher intrinsic hole mobility than its carbon-based analogue attributed to partial localization of the frontier orbitals induced by BN substitution, implying that BN-substituted aromatics might outperform their carbon analogues in organic electronics.[50] Nevertheless, all current reports focus on BN-fused PAHs annulated with electron-rich cyclic units.[51−53] The chemistry to fuse BN units into the frameworks of electron-deficient PAHs remains challenging and unexplored. This gap strongly encourages us to use PDI as an electron-deficient system to investigate the chemistry and properties of as-prepared BN-fused materials. Herein, we described the synthesis, characterization, and physical properties of a novel polycyclic 22e aromatic compound **PDI-1BN** consisting of azaborine and perlyene diimide, which is the first example about BN-annulation with highly electron-deficient PAHs. The as-prepared **PDI-1BN** not only shows very good stability but also displays high selectivity and sensitivity to fluoride ion. In addition, the OLED performance of **PDI-1BN** is also investigated.

Received: October 7, 2014
Published: December 1, 2014

   dx.doi.org/10.1021/jo502296z | J. Org. Chem. 2015, 80, 196−203

Scheme 1. Synthetic Route of Compound PDI-1BN

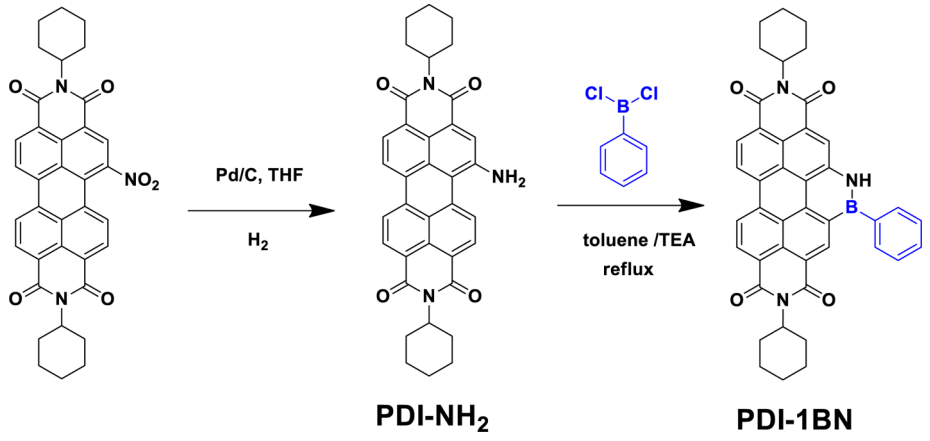

RESULTS AND DISCUSSION

Synthesis and Characterization. Compound **PDI-1BN** was prepared by reacting *N*,*N*-dicyclohexyl-(1-amino)perylene-3,4,9,10-tetracarboxylic acid bisimide (**PDI-NH$_2$**) with an dichlorophenylborane in dry toluene for 24 h under refluxing conditions using triethylamine as a base (Scheme 1). Compound **PDI-1BN** was obtained in 81% yield as a deep red solid after purification. The structure of compound **PDI-1BN** has been fully characterized through nuclear magnetic resonance (^{1}H and ^{13}C NMR), flourier transform infrared spectroscopy (FT-IR), high-resolution mass spectroscopy (HRMS), and thermogravimetric analysis (TGA) (see the Supporting Information). As shown in Figure S1, ^{1}H NMR spectroscopy of compound **PDI-1BN** showed the characteristic singlets at 9.43, 8.83, and 8.57 ppm corresponding to H_a, H_b, and H_c protons, whereas ^{13}C NMR spectroscopy displayed the characteristic peaks at 164.29, 163.97, 163.92, and 163.51 ppm, which can be assigned to four carbonyl carbons (Figure S2) (Supporting Information). **PDI-1BN** can dissolve in common organic solvents such as dichloromethane, chloroform, tetrahydrofuran (THF), and toluene, but shows poor solubility in dimethylformamide (DMF) and dimethyl sulfoxide (DMSO). TGA revealed the decomposition temperature (5% weight loss) as high as 402 °C for **PDI-1BN** (Figure S5, Supporting Information). Such a remarkable thermal stability is very promising for its future application in organic semiconductor devices.

The UV−vis absorption spectrum of compound **PDI-1BN** was depicted in Figure 1. It exhibited a strong absorption maximum at 529 nm and a shoulder of 494 nm, which was bathochromically shifted by about 60 nm compared to its C═C analogue.[36] This red-shifted phenomenon can be explained by the strong dipole moment of sp^2-type BN (1.84D) relative to C═C (0D).[45] Meanwhile, strong yellowish-green fluorescence with the emission wavelength at 540 nm was observed after excitation at 493 nm, while the carbon−carbon analogue emitted at 477 nm. The fluorescence quantum yield (0.81) in chloroform solution was measured using fluorescein as standard (Φf = 0.85, 0.1 M NaOH),[54] which was higher than that of its C═C analogue (φf = 0.77 in chloroform).[36] Clearly, the introduction of BN into PDIs could maintain its molecular rigidness but display dramatically different optical properties.

The electrochemical property was investigated using cyclic voltammetry method (Figure 2). Compound **PDI-1BN** underwent three chemically reversible reductive processes,

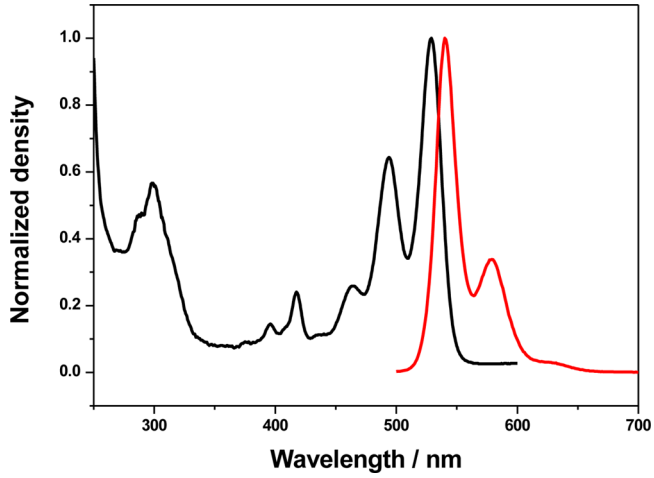

Figure 1. UV−vis and fluorescence spectra of compound **PDI-1BN** (10 μM in $CHCl_3$).

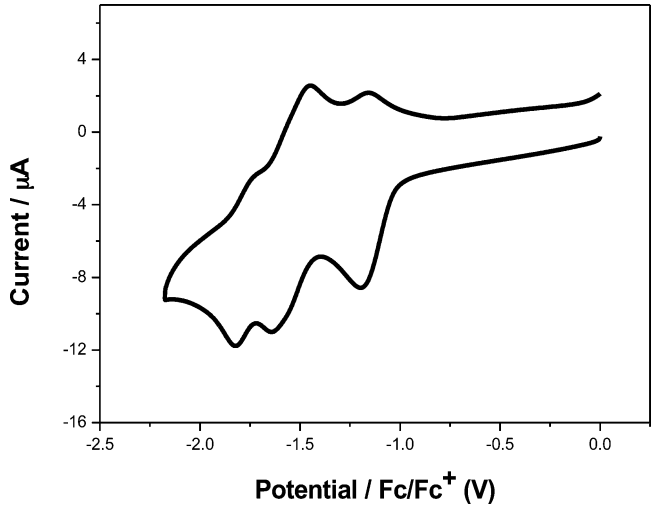

Figure 2. Cyclic voltammetry (CV) curve of compound **PDI-1BN**.

suggesting that monoanionic, dianionic, and trianionic derivatives may be accessible. The onset potential of the first reduction wave was −1.17 eV, so the lowest unoccupied molecular orbital (LUMO) energy level (E_{LUMO}) was determined to be −3.63 eV according to the equation of E_{LUMO} = −4.8 eV − E_{red}.[55a] Since the LUMO of the B-N

dx.doi.org/10.1021/jo502296z | J. Org. Chem. 2015, 80, 196−203

molecule (−3.63 eV) is between the PDI (−3.98 eV) and PDI-NH_2 (−3.33 eV),[55b,c] we believe that BN units could be slightly electron-rich and fusing a BN unit into PDI could slightly increase the LUMO energy level. In fact, the B atom might give relatively less contributions to LUMO comparing with an NH group.[55b,c] The band gap was estimated through optical maximum absorption (529 nm, E_g = 2.34 eV), so the highest occupied molecular orbital (HOMO) energy level (−5.97 eV) could be calculated according to the empirical formula: $E_{HOMO} = E_{LUMO} - E_g$.[56]

Theoretical Calculation. To understand the electronic structure of compound **PDI-1BN**, a theoretical investigation is conducted through molecular simulation. The molecular geometry of **PDI-1BN** in the ground state was fully optimized using density functional theory (DFT) at the B3LYP/6-31G* level, and the frontier molecular orbitals of **PDI-1BN** are shown in Figure 3. Evidently, the LUMO orbital is more delocalized

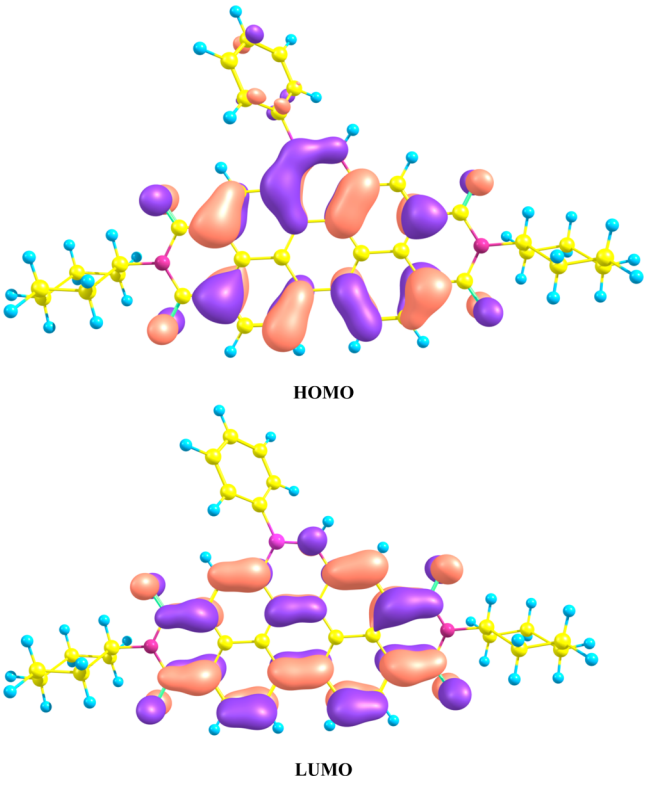

Figure 3. Wave functions for the HOMO and LUMO of **PDI-1BN**.

than the HOMO orbital. The B3LYP/6-31G* calculated energies of HOMO, LUMO, and band gap are −5.84, −3.24, and 2.60 eV, respectively, which are close to the experimental results (−5.97, −3.63, 2.34 eV).[57] Based on the B3LYP/6-31G* optimized geometry, B3PW91 single-point energy calculations were performed to obtain the energies of HOMO, LUMO, and band gap, and the calculated results are also reported in Table S1 (Supporting Information). The absolute energies of HOMO and LUMO orbitals and the atom coordinates of PDI-1BN in the ground state are also given in Tables S2 and S3 (Supporting Information), respectively.

Fluoride Sensing Ability. The anion-sensing properties of **PDI-1BN** were investigated upon adding 10 equiv of different anions. Figure 4 shows the changes of the UV−vis spectra of **PDI-1BN** (1×10^{-5} M in chloroform). The inset shows the corresponding color response of **PDI-1BN** with 12 different

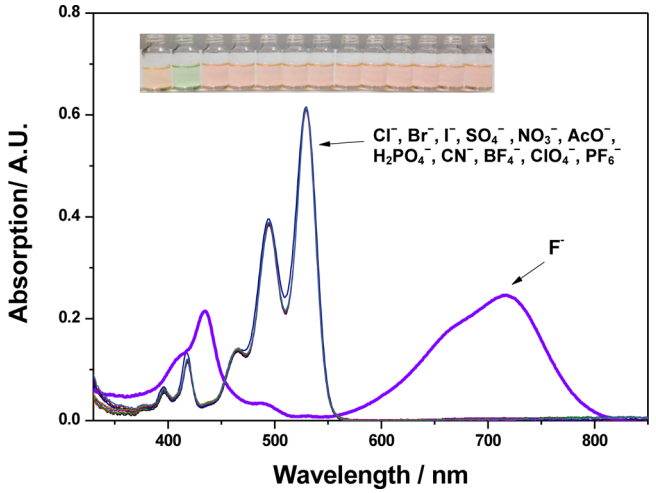

Figure 4. UV−vis spectral changes of compound **PDI-1BN** (10 μM in $CHCl_3$) observed upon addition of 10 equiv of different anions (TBA salt).

anions (F^-, Cl^-, Br^-, I^-, SO_4^-, NO_3^-, CH_3COO^-, $H_2PO_4^-$, CN^-, BF_4^-, ClO_4^-, and PF_6^-). Specifically, **PDI-1BN** showed no obvious response to all other anions except the fluoride anion. Only the acetate ion shows a slight affinity to **PDI-1BN** when more than 100 equiv of acetate anions was added. Moreover, fluorescence quenching was also observed upon adding 10 equiv of fluoride anions (Figure 5). The dramatic anion-specific response suggests that **PDI-1BN** is a highly selective colorimetric sensor to fluoride anion.

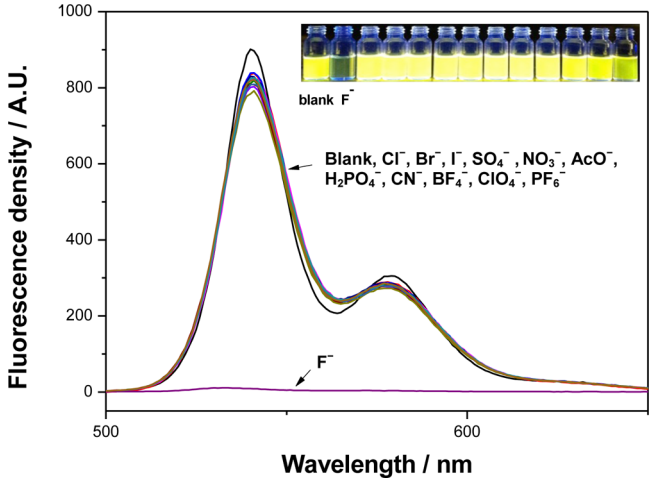

Figure 5. Fluorescence density changes of compound **PDI-1BN** (10 μM in $CHCl_3$) observed upon addition of 10 equiv of different anions (TBA salt).

Upon the addition of Bu_4NF (0−10.0 equiv), the intensity bands at 494 and 529 nm steadily decreased, and at the meanwhile, two new bands at 434 and 715 nm with two clear isobestic points were observed (Figure 6). Furthermore, when Bu_4NF reached 3 equiv, significant fluorescence quenching (~98%) was observed (Figure 7), which is attributed to the high charge density of fluoride anion. For all other anions, only smaller effects (<15% quenching) were observed even after the concentration reached 1000 equiv, suggesting that compound **PDI-1BN** presented a high sensitivity and selectivity for fluoride ion over other anions. In particular, the response of

dx.doi.org/10.1021/jo502296z | J. Org. Chem. 2015, 80, 196−203

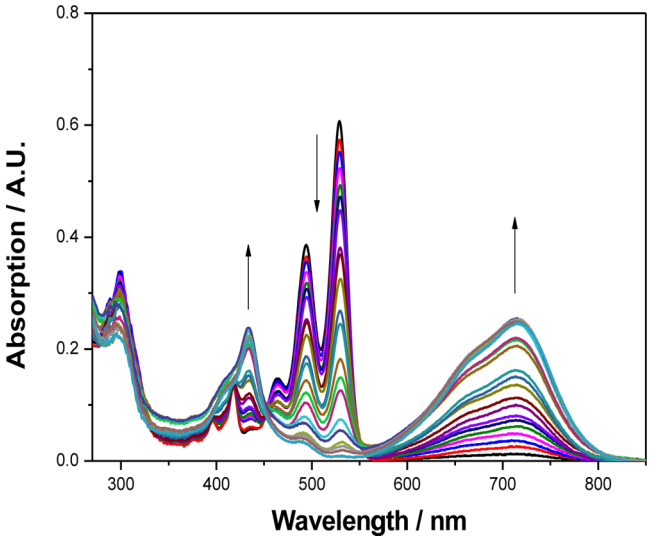

Figure 6. UV−vis spectral changes of compound **PDI-1BN** (10 μM in $CHCl_3$) observed upon addition of 0−10 equiv of TBAF in DMF.

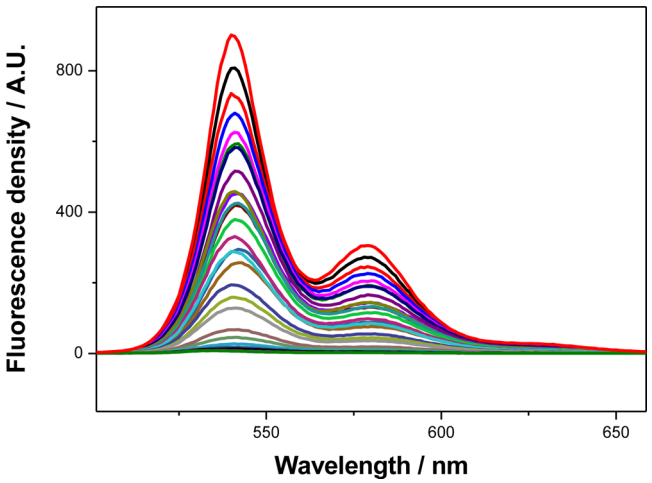

Figure 7. UV−vis spectral changes of compound **PDI-1BN** (10 μM in $CHCl_3$) observed upon addition of 0−10 equiv of TBAF in DMF.

PDI-1BN to fluoride was very fast, normally within 1 sec. The detection limitation was about 1.5 μM under our experimental conditions (Figure S6, Supporting Information).

To confirm the stoichiometry of the binding of the probe **PDI-1BN** with fluoride, Job's plots (continuous variation plots) analysis was carried out. The absorbance variation at 715 nm against the molar fraction of fluoride clearly showed the maxima with a molar fraction of 0.66, indicating a 2:1 stoichiometry (Figure S7, Supporting Information). The mechanism of the interaction between compound **PDI-1BN** and fluoride was further studied by ^{1}H NMR titration experiments (Figure 8). Upon the addition of 2.0 equiv of fluoride, the azaborazine NH proton completely vanished. Two single peaks of 9.48 ppm (H_a) and 8.64 ppm (H_c) shifted to high field of 8.67 and 8.07 ppm, respectively. This clearly suggests that the deprotonation of the azaborazine NH proton by fluoride leads to the obvious changes in absorption and fluorescence.

OLED Devices. To investigate the performance of **PDI-1BN** in OLEDs, we fabricated a series of OLEDs with structures of ITO/MoO_3 (2 nm)/TCTA (80 nm)/CBP: *X* wt % **PDI-1BN** (20 nm)/TPBi (40 nm)/LiF (1 nm)/Al (200 nm), where MoO_3 is the hole injection layer, TCTA is a hole transporting layer, and TPBi is the electron transporting layer. The weight ratios of **PDI-1BN** in CBP are 1, 5, 10, 15, and 100%, where 100% means the neat **PDI-1BN** layer. As shown in Figure 9a, with the concentration of **PDI-1BN** increased from 1% to 15%, the current density of the device shows some increase as well, which can be explained by the increased electron injection from TPBi into the EML due to the smaller electron injection barrier from TPBi into **PDI-1BN** compared with that of TPBi to CBP. For the neat **PDI-1BN** device, the current density is even higher, which indicates that **PDI-1BN** has better electron mobility than CBP. The inset of Figure 9a shows the *J*−*V* curves in log-linear scale. As can be seen, the voltages at which the current density increases drastically for all the devices are around 3.0 eV, which predicts that these five devices should have similar turn-on voltages for electron/hole recombination. However, as shown in Figure 9b, the turn-on voltages (at a luminance of 1 cd/m^2) for all five devices are quite different. The turn-on voltages are 3.5, 3.6, 3.7, and 3.8 V for the devices with doping ratios of 1, 5, 10, and 15%, respectively, while, for the neat **PDI-1BN** device, the turn-on voltage is around 6.8 V. In fact, this turn-on voltage cannot fully reflect the electron/hole recombination process, as the electron/hole recombination can happen at very low voltage, but the conversion efficiency of excitons to photons can be quite different.

In Figure 9c, as the doping ratio increases, the external quantum efficiency (EQE) decreases gradually. The maximum EQEs are 1.57, 1.19, 1.01, and 0.91% for the devices with the doping ratios of 1, 5, 10, and 15%, respectively. For the neat **PDI-1BN** device, the EQE is even lower and its maximum EQE is around 0.05%. The current efficiencies and power efficiencies for these devices show similar behavior as EQE. Considering

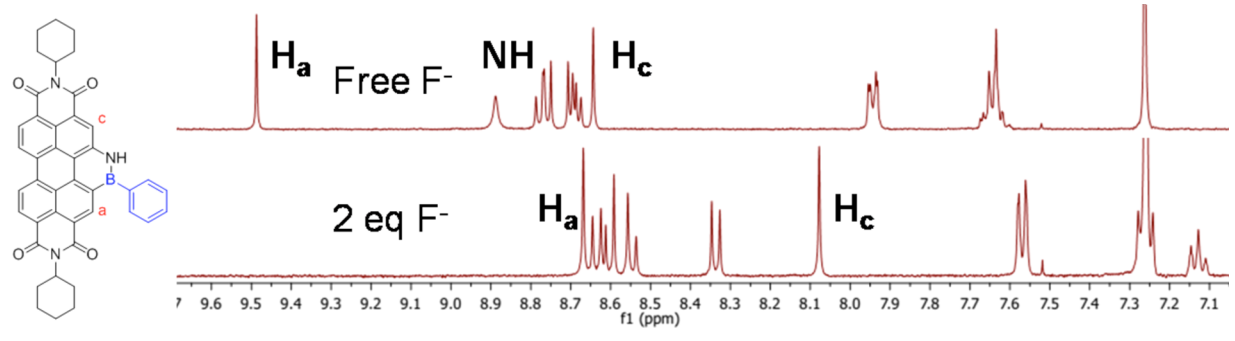

Figure 8. ^{1}H NMR spectra of compound **PDI-1BN** in $CDCl_3$ in the absence and presence of 2.0 equiv of TBAF.

dx.doi.org/10.1021/jo502296z | J. Org. Chem. 2015, 80, 196−203

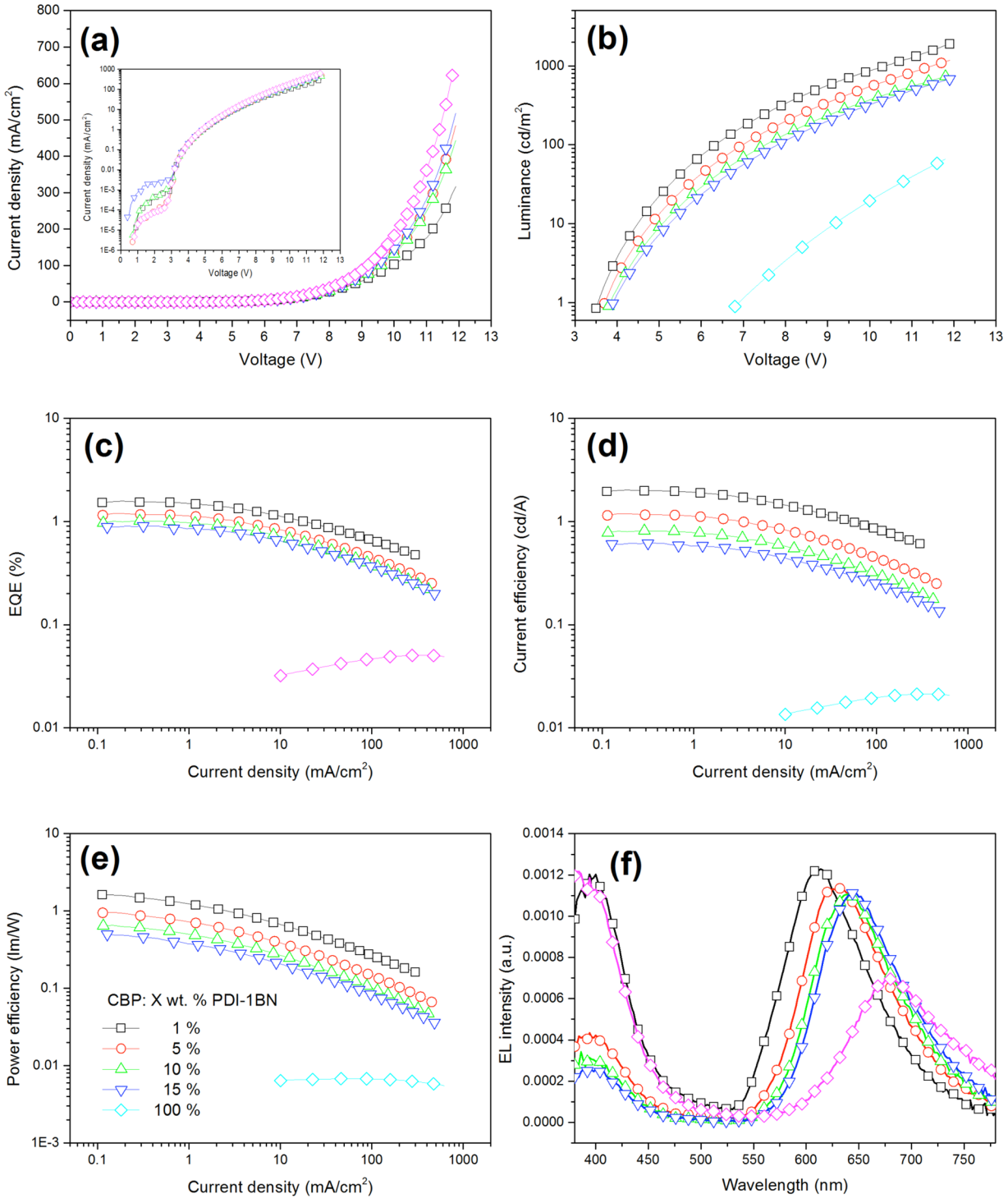

Figure 9. (a) Current density−voltage curves, (b) luminance−voltage curves, (c) external quantum efficiency curves, (d) current efficiency curves, (e) power efficiency curves, and (f) electroluminance spectra for the devices with **PDI-1BN** doping ratios of 1, 5, 10, 15, and 100%.

the PLQY of **PDI-1BN** in solution, the EQE is lower than expected (2%). The reduced EQE is due to the aggregation induced quenching (AIQ) process, which can be supported by the electroluminance spectra of these devices. As shown in Figure 9f, the emission peak shows continuous red-shifts as the doping ratio of **PDI-1BN** increases. The emission peaks are 616, 630, 636, 646, and 682 nm for the devices with doping ratios of 1, 5, 10, 15, and 100%, respectively. Compared with the PL peak (540 nm) of **PDI-1BN** solution, these EL peaks indicate that **PDI-1BN** will strongly aggregate in the film state. Also, the emission peak around 400 nm (Figure 9f), which comes from the host, is another evidence of **PDI-1BN** aggregation.

CONCLUSION

In summary, a new robust azaborazine-annulated perylene diimide (**PDI-1BN**) has been successfully synthesized through one concise intramolecular electrophilic arene borylation reaction. The as-prepared **PDI-1BN** has been fully charac-

dx.doi.org/10.1021/jo502296z | J. Org. Chem. 2015, 80, 196−203

terized by conventional spectroscopy techniques. The HOMO and LUMO energy levels obtained through DFT calculations are close to the experimental CV values. Interestingly, **PDI-1BN** can act as a highly sensitive and selective anion sensor for the detection of fluoride in chloroform solution among 12 anions (F^-, Cl^-, Br^-, I^-, SO_4^-, NO_3^-, CH_3COO^-, $H_2PO_4^-$, CN^-, BF_4^-, ClO_4^-, and PF_6^-), and the detection limitation could be as low as 1.5 μM. In addition, the as-prepared **PDI-1BN** has also been employed as an active element in OLEDs devices. We believe that our result could provide guidance for the design and synthesis of new azaborine-based polycyclic aromatic hydrocarbons.

EXPERIMENTAL SECTION

General Procedure. All synthetic precedures were performed under an argon atmosphere using standard Schlenk techniques. Dichloromethane, toluene, triethylamine, and dichloroethane were distilled from CaH_2 under an argon atmosphere. Other solvents and reactants were used without further purification. *N,N*-dicyclohexyl-(1-amino)perylene-3,4,9,10-tetracarboxylic acid bisimide (PDI-NH_2) was synthesized according to a reported procedure with slight modification.[58] ^{1}H NMR spectra were taken on a 400 MHz spectrometer, and chemical shifts (δ) are reported in ppm, using $CDCl_3$ (7.26 ppm) as an internal standard. ^{13}C NMR was recorded at a 100 MHz spectrometer. Matrix assisted laser desorption/ionization time-of-flight (MALDI-TOF) mass spectra were obtained on a TOF mass spectrometer. Thermogravimetric analysis (TGA) was carried out on a Thermogravimetric Analyzer at a heating rate of 5 °C/min up to 700 °C.

Synthesis Protocols. *Synthesis of N,N-Dicyclohexyl-(1-amino)-perylene-3,4,9,10-tetracarboxylic Acid Diimide (**PDI-NH_2**).* *N,N*-dicyclohexyl-(1-nitro)perylene-3,4,9,10-tetracarboxylic acid bisimide (1.5 g, 2.5 mmol), THF (150 mL), and Pd/C (dry, 10%, 150 mg) were added into a 250 mL two-neck flask, and degassed for 10 min by purging argon. Hydrogen was introduced into the sealed reaction system through a balloon, and the reaction was allowed to proceed at room temperature for 3 days. Then, the reaction mixture was filtered through a G4-sintered filter funnel and rinsed with THF until the filtrate became transparent. After removing solvent, a small amount of ethyl ether was added and the precipitate was filtered and dried in vacuum. The as-prepared crude product was used directly for the next step without further purification because of the instability of the amino in the air.

*Synthesis of N,N-Dicyclohexyl-1-aza-12-bora-benzoperylene-3,4,9,10-tetracarboxylic Acid Diimide (**PDI-1BN**).* Compound PDI-NH_2 (100 mg, 0.175 mmol), toluene (20 mL), dichlorophenylborane (Aldrich, 98%, 0.2 mL, 1.54 mmol), and triethylamine (0.5 mL) were mixed in a Schlenk tube under an argon atmosphere. The resulted mixture was refluxing for 24 h. After cooling to room temperature, the solvent was removed and the mixture was purified by flash silica gel chromatography using CH_2Cl_2/THF (200:1, V/V) as eluent, which yielded compound **PDI-1BN** as a red solid (93.2 mg, 81%). mp > 300 °C. ^{1}H NMR (400 MHz, $CDCl_3$, δ ppm) 9.43 (s, 1H), 8.83 (s, 1H), 8.69−8.62 (m, 3H), 8.57−8.55(m, 2H), 7.93−7.90 (m. 2H), 7.66−7.60 (m, 3H,) 5.12−5.16 (m, 2H), 2.66−2.58 (m, 4H), 1.96−1.77 (m, 10H), 1.57−1.41 (m, 6H). ^{13}C NMR (100 MHz, $CDCl_3$, δ ppm) 164.2, 163.9, 163.9, 163.5, 138.6, 137.7, 135.9, 134.0, 133.9, 132.1, 130.4, 129.7, 129.2, 128.8, 127.8, 124.7, 124.7, 124.3, 124.11, 123.7, 123.3, 123.1, 122.3, 121.5, 121.2, 117.2, 54.4, 54.1, 29.2, 26.6, 26.6, 25.56 25.4. FT-IR (KBr, cm^{-1}): 3461, 2931, 1670, 1655. HRMS: $(M + H)^+$, $C_{42}H_{35}BN_3O_4$, calcd, 656.2721; found 656.2747.

Anion sensor study: Stock solutions (1.0×10^{-5} M) of compound **PDI-1BN** were prepared in chloroform, and a stock solution of the guest (1.0×10^{-3} M) was prepared by dissolving F^-, Cl^-, Br^-, I^-, SO_4^-, NO_3^-, $H_2PO_4^-$, PF_6^-, BF_4^-, ClO_4^-, CN^-, and Ac^- (as salt of tetra-*n*-butylammonia) in *N,N*-dimethylamide (DMF). The general procedure for the UV−vis and fluorescence sensor studies involved making sequential additions of titrant (anionic guest) using pipettes to a 2 mL of the host stock solutions in the spectrometric cell. The value of the stability constant for the complex was calculated by a nonlinear curve fitness as the reported method.[4f]

Cyclic Voltammetry (CV) Measurements. Electrochemistry was carried out under argon at room temperature by employing glassy carbon (diameter: 1.6 mm; area: 0.02 cm^2) and two platinum wires as working electrode, counter electrode, and reference electrode, respectively. Tetrabutyl-ammonium hexafluorophosphate (0.1 M) in dry dichloroethane was used as an electrolyte. The scanning rate is 0.05 V/s. The potential was externally calibrated against the ferrocene/ferrocenium couple assuming HOMO of Fc/Fc^+ to be 4.88 eV, and the potential of Fc/Fc^+ in our measured condition was 0.31 V.

Fluorescence Quantum Yield Measurements. All spectroscopic measurements of the compound **PDI-1BN** were performed in chloroform using a cuvette with a 1 cm path length at 25 ± 0.1 °C. For each experiment, the slit width was 1.0 nm for both excitation and emission. Fluorescence quantum yield measurements were performed on a fluorometer and UV−vis instrument. The absorbance spectra were measured within an maximum absorbance close to 0.05 (l = 10 cm). Relative quantum efficiency was obtained according to the following equation

$$\Phi_{sample} = \Phi_{standard}(A_{standard}/A_{sample})(F_{sample}/F_{standard})(n_{sample}^2/n_{standard}^2)$$

where "Φ" is the quantum yield, "A" is the absorbance at the excited wavelength, "F" is the integrated area under the emission curve, and "n" is the refractive index of the solvent used (chloroform, 1.445; water, 1.333). Fluorescein (Φ_f = 0.85) in 0.1 M aqueous NaOH was used as fluorescence standard, and the excited wavelength is 508 nm, which is the intersection point of fluorescein and compound **PDI-1BN** in low concentration.

Fabrication of OLED Devices. All devices were fabricated on commercial ITO-coated glass substrates (15 Ω/sq). The ITO substrates were treated in order by ultrasonic bath sonication of detergent, deionized water, acetone, and isopropanol, each with a 20 min interval. Then, the ITO substrates were dried with nitrogen gas and baked in an oven at 80 °C for 30 min. After that, oxygen plasma treatment was carried out in a plasma cleaner. Subsequently, the substrates were transferred into a thermal evaporator, where the organic, inorganic, and metal functional layers were grown layer by layer at a base pressure of less than 4×10^{-4} Pa. The evaporation rates were monitored with several quartz crystal microbalances located above the crucibles and thermal boats. For organic semiconductors and metal oxides, the typical evaporation rates were about 0.1 nm/s, whereas, for aluminum, the evaporation rate was about 1−5 nm/s. The intersection of Al and ITO forms a 1 mm × 1 mm active device area. $J-V$ and $L-V$ data were collected with a source meter and a calibrated Si-photodetector with a customized Labview program. The electroluminance spectrum was measured with a spectrometer.

ASSOCIATED CONTENT

Supporting Information

The original ^{1}H NMR, ^{13}C NMR, MALDI-TOF, TGA, and FT-IR. This material is available free of charge via the Internet at http://pubs.acs.org.

AUTHOR INFORMATION

Corresponding Authors

*E-mail: EXWSun@ntu.edu.sg (X.W.S.).
*E-mail: QCZhang@ntu.edu.sg (Q.Z.).

Notes

The authors declare no competing financial interest.

ACKNOWLEDGMENTS

The authors would like to thank Dr. Long Guankui for partial calculation. Q.Z. acknowledges financial support from AcRF

Tier 1 (RG 16/12) and Tier 2 (ARC 20/12 and ARC 2/13) from MOE, and the CREATE program (Nanomaterials for Energy and Water Management) from NRF, Singapore. G.L. acknowledges the National Natural Science Foundation of China (NSFC; grant 21102150).

REFERENCES

(1) Houk, K. N.; Lee, P. S.; Nendel, M. *J. Org. Chem.* **2001**, *66*, 5517.
(2) Bendikov, M.; Duong, H. M.; Starkey, K.; Houk, K. N.; Carter, E. A.; Wudl, F. *J. Am. Chem. Soc.* **2004**, *126*, 7416.
(3) Bendikov, M.; Wudl, F.; Perepichka, D. F. *Chem. Rev.* **2004**, *104*, 4891.
(4) Anthony, J. E. *Chem. Rev.* **2006**, *106*, 5028.
(5) Anthony, J. E. *Angew. Chem., Int. Ed.* **2008**, *47*, 452.
(6) Zade, S. S.; Bendikov, M. *Angew. Chem., Int. Ed.* **2010**, *49*, 4012.
(7) Payne, M. M.; Parkin, S. R.; Anthony, J. E. *J. Am. Chem. Soc.* **2005**, *127*, 8028.
(8) (a) Chun, D.; Cheng, Y.; Wudl, F. *Angew. Chem., Int. Ed.* **2008**, *47*, 8380. (b) Gu, P.-Y.; Zhou, F.; Gao, J.; Li, G.; Wang, C.; Xu, Q. F.; Zhang, Q.; Lu, J. *J. Am. Chem. Soc.* **2013**, *135*, 14086. (c) Wu, Y.; Yin, Z.; Xiao, J.; Liu, Y.; Wei, F.; Tan, K. J.; Kloc, C.; Huang, L.; Yan, Q.; Hu, F.; Zhang, H.; Zhang, Q. *ACS Appl. Mater. Interfaces* **2012**, *4*, 1883. (d) Xiao, J.; Malliakas, C. D.; Liu, Y.; Zhou, F.; Li, G.; Su, H.; Kanatzidis, M. G.; Wudl, F.; Zhang, Q. *Chem.—Asian J.* **2012**, *7*, 672.
(9) Kaur, I.; Stein, N. N.; Kopreski, R. P.; Miller, G. P. *J. Am. Chem. Soc.* **2009**, *131*, 3424.
(10) Kaur, I.; Jazdzyk, M.; Stein, N. N.; Prusevich, P.; Miller, G. P. *J. Am. Chem. Soc.* **2010**, *132*, 1261.
(11) (a) Li, J.; Zhang, Q. *Synlett* **2013**, *24*, 686. (b) Xiao, J.; Yang, B.; Wong, J. I.; Liu, Y.; Wei, F.; Tan, K. J.; Teng, X.; Wu, Y.; Huang, L.; Kloc, C.; Boey, F.; Ma, J.; Zhang, H.; Yang, H.; Zhang, Q. *Org. Lett.* **2011**, *13*, 3004. (c) Zhang, Q.; Xiao, J.; Yin, Z. Y.; Duong, H. M.; Qiao, F.; Boey, F.; Hu, X.; Zhang, H.; Wudl, F. *Chem.—Asian. J.* **2011**, *6*, 856.
(12) Purushothaman, B.; Bruzek, M.; Parkin, S. R.; Miller, A. F.; Anthony, J. E. *Angew. Chem., Int. Ed.* **2011**, *50*, 7013.
(13) Watanabe, M.; Chang, Y. J.; Liu, S. W.; Chao, T. H.; Goto, K.; Islam, M. M.; Yuan, C. H.; Tao, Y. T.; Shinmyozu, T.; Chow, T. J. *Nat. Chem.* **2012**, *4*, 574.
(14) (a) Xiao, J. C.; Duong, H. M.; Liu, Y.; Shi, W. X.; Ji, L.; Li, G.; Li, S. Z.; Liu, X. W.; Ma, J.; Wudl, F.; Zhang, Q. *Angew. Chem., Int. Ed.* **2012**, *51*, 6094. (b) Li, G.; Duong, H. M.; Zhang, Z.; Xiao, J.; Liu, L.; Zhao, Y.; Zhang, H.; Huo, F.; Li, S.; J. Ma, J.; F. Wudl, F.; Zhang, Q. *Chem. Commun.* **2012**, *48*, 5974.
(15) (a) Würthner, F. *Chem. Commun.* **2004**, 1564. (b) Jones, B. A.; Facchetti, A.; Wasielewski, M. R.; Marks, T. J. *J. Am. Chem. Soc.* **2007**, *129*, 15259. (c) Chen, Z.-J.; Wang, L.-M.; Zou, G.; Zhang, L.; Zhang, G. J.; Cai, X. F.; Teng, M. S. *Dyes Pigm.* **2012**, *94*, 410.
(16) Oh, J. H.; Lee, H. W.; Mannsfeld, S.; Stoltenberg, R. M.; Jung, E.; Jin, Y. W.; Kim, J. M.; Yoo, J. B.; Bao, Z. N. *Proc. Natl. Acad. Sci. U.S.A.* **2009**, *106*, 6065.
(17) Zhou, E. J.; Cong, J. Z.; Wei, Q. S.; Tajima, K.; Yang, C. H.; Hashimoto, K. *Angew. Chem., Int. Ed.* **2011**, *50*, 2799.
(18) Zhao, J.; Wong, J. I.; Wang, C.; Gao, J.; Ng, V. Z. Y.; Yang, H. Y.; Loo, S. C. J.; Zhang, Q. *Chem.—Asian J.* **2013**, *8*, 665−669.
(19) Zhang, X.; Lu, Z. H.; Ye, L.; Zhan, C. L.; Hou, J. H.; Zhang, S. Q.; Jiang, B.; Zhao, Y.; Huang, J. H.; Zhang, S. L.; Liu, Y.; Shi, Q.; Liu, Y. Q.; Yao, J. N. *Adv. Mater.* **2013**, *25*, 5791.
(20) Jones, B. A.; Ahrens, M. J.; Yoon, M. H.; Facchetti, A.; Marks, T. J.; Wasielewski, M. R. *Angew. Chem., Int. Ed.* **2004**, *43*, 6363.
(21) Zhan, X. W.; Tan, Z. A.; Domercq, B.; An, Z. S.; Zhang, X.; Barlow, S.; Li, Y. F.; Zhu, D. B.; Kippelen, B.; Marder, S. R. *J. Am. Chem. Soc.* **2007**, *129*, 7246.
(22) Anthony, J. E.; Facchetti, A.; Heeney, M.; Marder, S. R.; Zhan, X. W. *Adv. Mater.* **2010**, *22*, 3876.
(23) Jung, B. J.; Tremblay, N. J.; Yeh, M. L.; Katz, H. E. *Chem. Mater.* **2011**, *23*, 568.
(24) Law, K. Y. *Chem. Rev.* **1993**, *93*, 449.
(25) Zhao, J.; Wong, J. I.; Gao, J.; Li, G.; Xing, G.; Zhang, H.; Sum, T. C.; Yang, H. Y.; Zhao, Y.; Kjelleberg, S. L. A.; Huang, W.; Loo, S. C. J.; Zhang, Q. *RSC Adv.* **2014**, *4*, 17822.
(26) Pschirer, N. G.; Kohl, C.; Nolde, T.; Qu, J. Q.; Mullen, K. *Angew. Chem., Int. Ed.* **2006**, *45*, 1401.
(27) Rohr, U.; Schlichting, P.; Bohm, A.; Gross, M.; Meerholz, K.; Brauchle, C.; Mullen, K. *Angew. Chem., Int. Ed.* **1998**, *37*, 1434.
(28) Muller, S.; Mullen, K. M. *Chem. Commun.* **2005**, 4045.
(29) Avlasevich, Y.; Muller, S.; Erk, P.; Mullen, K. *Chem.—Eur. J.* **2007**, *13*, 6555.
(30) Yan, Q. F.; Zhao, D. H. *Org. Lett.* **2009**, *11*, 3426.
(31) Yuan, Z. Y.; Xiao, Y.; Qian, X. H. *Chem. Commun.* **2010**, *46*, 2772.
(32) Yuan, Z. Y.; Xiao, Y.; Yang, Y.; Xiong, T. *Macromolecules* **2011**, *44*, 1788.
(33) Miao, Q.; Nguyen, T. Q.; Someya, T.; Blanchet, G. B.; Nuckolls, C. *J. Am. Chem. Soc.* **2003**, *125*, 10284.
(34) Wood, T. K.; Piers, W. E.; Keay, B. A.; Parvez, M. *Angew. Chem., Int. Ed.* **2009**, *48*, 4009.
(35) Wood, T. K.; Piers, W. E.; Keay, B. A.; Parvez, M. *Chem.—Eur. J.* **2010**, *16*, 12199.
(36) Langhals, H.; Kirner, S. *Eur. J. Org. Chem.* **2000**, 365.
(37) Li, Y. J.; Li, Y. L.; Li, J. B.; Li, C. H.; Liu, X. F.; Yuan, M. J.; Liu, H. B.; Wang, S. *Chem.—Eur. J.* **2006**, *12*, 8378.
(38) Jaggi, M.; Blum, C.; Marti, B. S.; Liu, S. X.; Leutwyler, S.; Decurtins, S. *Org. Lett.* **2010**, *12*, 1344.
(39) Choi, H.; Paek, S.; Song, J.; Kim, C.; Cho, N.; Ko, J. *Chem. Commun.* **2011**, *47*, 5509.
(40) Schmidt, C. D.; Lang, N. N.; Jux, N.; Hirsch, A. *Chem.—Eur. J.* **2011**, *17*, 5289.
(41) Qian, H. L.; Liu, C. M.; Wang, Z. H.; Zhu, D. B. *Chem. Commun.* **2006**, 4587.
(42) Qian, H. L.; Yue, W.; Zhen, Y. G.; Di Motta, S.; Di Donato, E.; Negri, F.; Qu, J. Q.; Xu, W.; Zhu, D. B.; Wang, Z. H. *J. Org. Chem.* **2009**, *74*, 6275.
(43) Liu, Z. Q.; Marder, T. B. *Angew. Chem., Int. Ed.* **2008**, *47*, 242.
(44) Bosdet, M. J. D.; Piers, W. E. *Can. J. Chem.* **2009**, *87*, 8.
(45) Campbell, P. G.; Marwitz, A. J. V.; Liu, S. Y. *Angew. Chem., Int. Ed.* **2012**, *51*, 6074.
(46) Lu, J. S.; Ko, S. B.; Walters, N. R.; Kang, Y.; Sauriol, F.; Wang, S. N. *Angew. Chem., Int. Ed.* **2013**, *52*, 4544.
(47) Araneda, J. F.; Neue, B.; Piers, W. E. *Angew. Chem., Int. Ed.* **2012**, *51*, 9977.
(48) Saito, S.; Matsuo, K.; Yamaguchi, S. *J. Am. Chem. Soc.* **2012**, *134*, 9130.
(49) Zhou, Z. G.; Wakamiya, A.; Kushida, T.; Yamaguchi, S. *J. Am. Chem. Soc.* **2012**, *134*, 4529.
(50) Hatakeyama, T.; Hashimoto, S.; Oba, T.; Nakamura, M. *J. Am. Chem. Soc.* **2012**, *134*, 19600.
(51) Bosdet, M. J. D.; Jaska, C. A.; Piers, W. E.; Sorensen, T. S.; Parvez, M. *Org. Lett.* **2007**, *9*, 1395.
(52) Wang, X. Y.; Zhang, F.; Liu, J.; Tang, R. Z.; Fu, Y. B.; Wu, D. Q.; Xu, Q.; Zhuang, X. D.; He, G. F.; Feng, X. L. *Org. Lett.* **2013**, *15*, 5714.
(53) Wang, X. Y.; Zhuang, F. D.; Wang, R. B.; Wang, X. C.; Cao, X. Y.; Wang, J. Y.; Pei, J. *J. Am. Chem. Soc.* **2014**, *136*, 3764.
(54) Shie, J. J.; Liu, Y. C.; Lee, Y. M.; Lim, C.; Fang, J. M.; Wong, C. H. *J. Am. Chem. Soc.* **2014**, *136*, 9953.
(55) (a) Love, J. A.; Nagao, I.; Huang, Y.; Kuik, M.; Gupta, V.; Takacs, C. J.; Coughlin, J. E.; Qi, L.; van der Poll, T. S.; Kramer, E. J.; Heeger, A. J.; Nguyen, T. Q.; Bazan, G. C. *J. Am. Chem. Soc.* **2014**, *136*, 3597. (b) Tsai, H.-Y.; Chen, K.-Y. *J. Lumin.* **2014**, *149*, 103. (c) Jiménez, A. J.; Lin, M.-J.; Burschka, C.; Becker, J.; Settels, V.; Engels, B.; Würthner, F. *Chem. Sci.* **2014**, *5*, 608.
(56) Li, G.; Miao, J. W.; Cao, J.; Zhu, J.; Liu, B.; Zhang, Q. *Chem. Commun.* **2014**, *50*, 7656.
(57) Frisch, M. J.; Trucks, G. W.; Schlegel, H. B.; Scuseria, G. E.; Robb, M. A.; Cheeseman, J. R.; Scalmani, G.; Barone, V.; Mennucci, B.; Petersson, G. A.; Nakatsuji, H.; Caricato, M.; Li, X.; Hratchian, H. P.; Izmaylov, A. F.; Bloino, J.; Zheng, G.; Sonnenberg, J. L.; Hada, M.;

Ehara, M.; Toyota, K.; Fukuda, R.; Hasegawa, J.; Ishida, M.; Nakajima, T.; Honda, Y.; Kitao, O.; Nakai, H.; Vreven, T.; Montgomery, J. A., Jr.; Peralta, J. E.; Ogliaro, F.; Bearpark, M.; Heyd, J. J.; Brothers, E.; Kudin, K. N.; Staroverov, V. N.; Kobayashi, R.; Normand, J.; Raghavachari, K.; Rendell, A.; Burant, J. C.; Iyengar, S. S.; Tomasi, J.; Cossi, M.; Rega, N.; Millam, M. J.; Klene, M.; Knox, J. E.; Cross, J. B.; Bakken, V.; Adamo, C.; Jaramillo, J.; Gomperts, R.; Stratmann, R. E.; Yazyev, O.; Austin, A. J.; Cammi, R.; Pomelli, C.; Ochterski, J. W.; Martin, R. L.; Morokuma, K.; Zakrzewski, V. G.; Voth, G. A.; Salvador, P.; Dannenberg, J. J.; Dapprich, S.; Daniels, A. D.; Farkas, Ö.; Foresman, J. B.; Ortiz, J. V.; Cioslowski, J.; Fox, D. J. *Gaussian 09*; Gaussian, Inc.: Wallingford, CT, 2009.

(58) Chen, K. Y.; Fang, T. C.; Chang, M. J. *Dyes Pigm.* **2012**, *92*, 517.

dx.doi.org/10.1021/jo502296z | *J. Org. Chem.* 2015, 80, 196−203